

Lecture Notes
in Geoinformation and Cartography

LNG&C

Martin Breunig · Mulhim Al-Doori
Edgar Butwilowski · Paul V. Kuper
Joachim Benner · Karl Heinz Haefele *Editors*

3D Geoinformation Science

The Selected Papers of the 3D GeoInfo
2014

 Springer

A Hybrid Approach Integrating 3D City Models, Remotely Sensed SAR Data and Interval-Valued Fuzzy Soft Set Based Decision Making for Post Disaster Mapping of Urban Areas

Iftikhar Ali, Aftab Ahmed Khan, Salman Qureshi, Mudassar Umar, Dagmar Haase and Ihab Hijazi

Abstract This chapter introduces a novel technique for post-disaster mapping and disaster scale estimation based on an integrated framework of SAR remote sensing and a 3D city model database, optical remote sensing imagery is used for validation purpose. SAR based urban damage detection is well established and has been used for many years. We have showed that how the existing 3D City Model can be updated with the information extracted from satellite remote sensing data. The third dimension will play a very crucial role in evacuation rout planning of damaged or affected buildings. In this study in the proposed–three-level (L_1 , L_2 , L_3)–model damage assessment information is integrated with the semantic knowledge of 3D city models in order to better organize the search and rescue operation. L_1 includes

[I. Ali](#) (✉)

Department of Geography, University College Cork, Cork, Ireland
e-mail: iffi.math@gmail.com

A.A. Khan

Technical University Munich, Munich, Germany
e-mail: aftab.khan@tum.de

[S. Qureshi](#) · [D. Haase](#)

Department of Geography, Humboldt University of Berlin, Unter den Linden, Berlin, Germany
e-mail: salman.qureshi@geo.hu-berlin.de

[D. Haase](#)

e-mail: dagmar.haase@ufz.de

M. Umar

Department of Remote Sensing and Geoinformatics, Institute of Space Technology, 75270 Karachi, Pakistan
e-mail: mudassar_bzu@yahoo.com

[I. Hijazi](#)

An-Najah University, Nablus, Palestine
e-mail: eehab@najah.edu

remotely sensed Synthetic Aperture Radar (SAR) space-borne data collection from the affected areas; L_2 includes a change detection process; and L_3 includes the estimation of the most affected building(s). Using this model, we show how the day-night image acquisition capability of a SAR sensor and semantic information from a 3D city model can be effectively used for post disaster mapping for rapid search and rescue operations. For L_1 , the combination of very high resolution SAR data and a 3D city model in CityGML format is used. L_2 works under predefined conditions to detect the types of changes that have occurred. In L_3 , an interval-valued fuzzy soft set theory method is proposed with which to estimate the scale of damage to the affected structures (buildings). In this study, we show the potential application of existing 3D city models (with semantic knowledge) in combination with SAR remote sensing for post disaster management activities, especially for search and rescue operations.

Keywords Urban remote sensing · Change detection · CityGML · Hazard mapping · Spatial analysis

1 Introduction

Urban areas with high concentration of people and multi-story residential apartments may result in high numbers of casualties in a building collapse following an earthquake. Earthquakes are highly unpredictable events, so that early warnings are required for successful evacuation ([Kagan 1997](#)). Earthquakes belong to the most deadly and destructive class of disasters where the delay in response could cause increase in number of casualties. With the rate of urbanization increasing as a result of population (and/or economic) growth and industrialization, global warming is also increasing. In future, for natural disasters management, more efficient, scientifically reliable and rapid search and rescue techniques will be required.

During disasters (earthquakes) in highly populated urban areas, the response time for emergency services is a crucial factor and should be optimized, while at the same time, the process of identification of damaged areas needs to be more fast, precise and as early as possible ([Trianni and Gamba 2009](#)). In the past, traditional methods such as aerial imagery and visual image interpretation ([Lu et al. 1998](#)) have been used for damage detection. For example, [Suga et al. \(2001\)](#) used InSAR data to detect urban damages and land displacement. Since the early 1990s, airborne laser scanning has been actively used for the change detection ([Martin and Bernhard 2010](#); [Murakami et al. 1999](#); [Vogtle and Steinle 2004](#)). In earthquakes in highly populated cities, the rapid estimation of potential damage and the detection of affected areas on a large scale have been a great challenge. Despite their advantages, the techniques that have traditionally been used have several limitations. More recently cities (and, more specifically, buildings) are now being analyzed in 3D virtual reality environment using semantic information from these

structures. The use of semantic 3D building models with international open standards such as CityGML and Industry Foundation Classes (IFC) has become very common. In recent years, many cities throughout the world have been switched to these international standards to support semantics and efficient visualization and to fulfill the challenging demands of users. CityGML is a common semantic information model for the representation, storage, and exchange of 3D urban objects based on the XML format (Kolbe et al. 2005). CityGML is implemented as an application schema of Geography Markup Language version 3.1.1 (GML3) (Kolbe et al. 2005) and is an international standard for the representation and exchange of semantic 3D city models (CityGML 2014; Gröger et al. 2008; Kolbe 2009). CityGML-based 3D city models work as the central information hub for various domains, such as tourism, environmental projection, urban planning, and navigation (Kolbe 2009). From a disaster management perspective, 3D city models in CityGML contain rich information, representing semantics, geometry, topology, and appearance (Kolbe et al. 2005), and objects can be represented at up to five levels of detail (LOD) (Kolbe 2009). Kolbe et al. (2005, 2009) gives a comprehensive overview of 3D city modeling and CityGML.

Remote sensing is another way of gathering information at a large scale. Recent development in earth observation sensors has made it possible to acquire high-resolution data at large scale. COSMO-SkyMed (Italian) and TerraSAR-X (German) are very high-resolution X-band Earth observation systems that are equipped with multi-acquisition modes, and they have large wide swath image acquisition capability. COSMO-SkyMed has a revisit time of ≈ 4.5 h with full constellation of four satellites, whereas TerraSAR-X has an 11-day revisit time. In the future, such sensors could be used for near real time monitoring activities. In the field of remote sensing, the major constraint is bad weather conditions; in such cases, SAR is the only reliable source of acquiring wide-swath and multi-temporal imagery. Number of studies has been done on the utilization of SAR data for the detection of change/damages caused by earthquake (Brunner et al. 2010; Dell'Acqua and Gamba 2012; Dell'Acqua et al. 2010, 2009; Dong and Shan 2013; Park et al. 2013; Tong et al. 2013; Trianni and Gamba 2009).

To the best of our knowledge, there is no framework that exploits the existing *3D Semantic City Model* and the SAR remotely sensed data for disaster management and mapping. The objective of this paper was to establish the feasibility of the mechanism that combines remotely sensed SAR data and a 3D Semantic City Model database, so that, in any disaster, the database for each building in a 3D Semantic City Model can be updated with additional information, and then query based semantic filtering (Kolbe et al. 2005) of damaged buildings can be used. Soft sets, fuzzy sets and fuzzy soft sets are the recent methods that have been developed and have matured to address the uncertainties present in real world situations (Chetia and Das 2010). In this paper, we propose the application of *interval-valued fuzzy soft sets* for the estimation of the scale of damage; a detailed description is provided in Sect. 5.3.

Table 1 Data used for this study

Sensors	Date	Event	Specifications
TerraSAR-X	05-12-2007	Pre-event (X_{t_1})	Mode: SpotLight, polarization: HH, incidence angle: 39.8°
TerraSAR-X	02-10-2011	Post-event (X_{t_2})	Mode: SpotLight, polarization: HH, incidence angle: 39.8°
QuickBird	11-11-2007	Pre-event (X_{t_1})	Mode: PAN
QuickBird	09-10-2011	Post-event (X_{t_2})	Mode: PAN

2 Data Used, Study Area and Preprocessing

The area under investigation is San Francisco, USA. The TerraSAR-X image pair was received at the L1B product level with a pixel spacing of 0.45 and 0.87 m in the slant range and azimuth, respectively. One image from each of QuickBird and WorldView-2 (PAN format) was used for cross check/validation. Table 1 shows the details of the data used.

To obtain square ground pixels, the SAR images were multi-looked. The images were co-registered, and a subset was taken to expedite the processing chain. Following the multi-looked and co-registration, an enhanced lee filter was applied to reduce the speckle effect. Geo-coding and radiometric correction were applied, and the average value of the backscattering coefficient was calculated (on a logarithmic scale) by overlaying the digital shape files of the building footprint. The image log ratio [$X_{LR} = \log(X_{t_2}/X_{t_1})$] technique was applied for the identification of changes. Other change detection methods can be used for change detection analysis (Lu et al. 2004). The scheme for the preprocessing steps of the TerraSAR-X images is illustrated in Fig. 1.

3 Methodology

3.1 Proposed Model

The LoD3 (level of detail) is sufficient for the proposed methodology where the building's architectural information like height, use (commercial or residential) number of stories are given; which are very crucial for search and rescue operations.

We divided our model theoretically into three levels of implementation, which are

- L₁ Space-borne data collection—information gathering regarding the affected areas
- L₂ Change detection types (CDT)—identification of the affected area
- L₃ Prediction—estimation of possible damage type and scale based on updated database

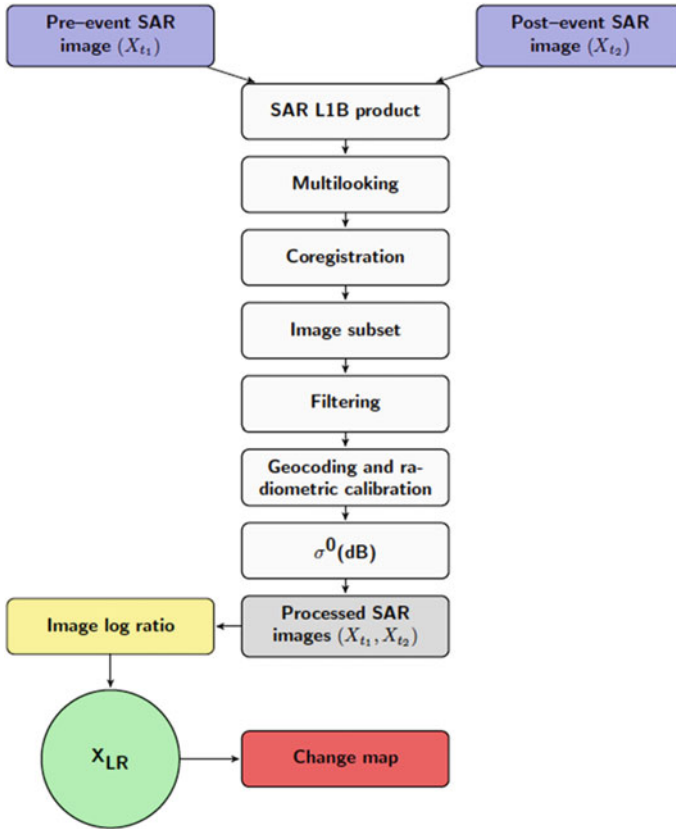


Fig. 1 Flowchart for SAR data preprocessing

A detailed description of each of these levels is given below (Sects. 3.2, 3.3 and 3.4).

3.1.1 Workflow of Proposed Model

The proposed model (Fig. 2) will start from Level L_1 where the labels (numbering in red color in Fig. 2) **1** (remote sensing data) and **4** (3D City Model database) represent the input data required for this model. After preprocessing the remote sensing data (label **2**) building footprints will be converted to ROIs (label **5–6**) in order to calculate the average signal backscatter for these ROIs (label **3**) and 3D City Model database (label **4**) will be updated with the pre and post event signal backscatter information for each building (this step does not mean that from now to onward model is fully shifting from 3D to 2D; rather this is just the one information extracted from 3D City Model in order to further update the existing 3D City

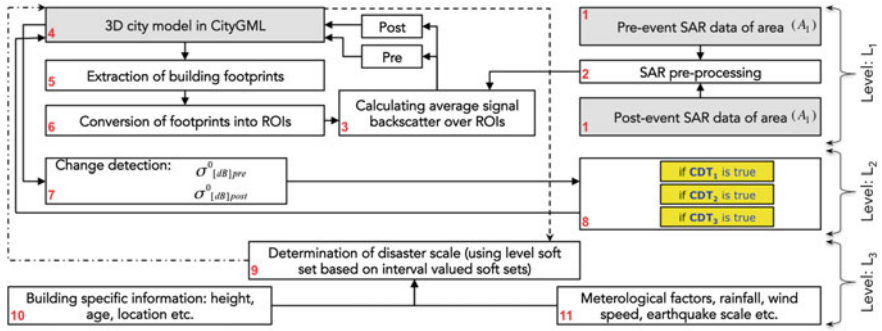


Fig. 2 L₁, L₂ and L₃ are the three levels of proposed model

Model). In the next step both pre and post SAR backscatter will be further use for the change detection (label 7) and classification of buildings in the database into destroyed, no change and new construction (label 8). In the final step information about destroyed (affected) in 3D City Model (label 4) along with meteorological (label 11) and other building related information (label 10) would be used in *interval-valued fuzzy soft set* algorithm (label 9) in order to prioritize the damage scale of each building.

3.2 Level L₁: Space-Borne Data Collection

The basic data requirements for L1 and this proposed model are a 3D city model and spaceborne VHR-SAR imagery. First, the footprints of all buildings (or the most important residential skyscrapers) were selected, and then these footprints were converted to regions of interest (ROIs). The pre-event SAR image acquisition at time t_1 was used in combination with the ROIs to calculate the average back scattering value (σ^0) over each ROI (representing building footprints). An attribute table for each building, containing semantic and other building related information, was edited to include two additional attributes: the pre-event ($\sigma^0_{[dB]pre}$) value and the post-event ($\sigma^0_{[dB]post}$) value. If an event (earthquake) happened at time t_1 , then the SAR image acquired after the event is represented as t_2 . Using the same ROIs, which were used to calculate pre-event ($\sigma^0_{[dB]pre}$) values, the post-event ($\sigma^0_{[dB]post}$) values were calculated and were stored in the edited attribute table of the 3D building model. In Fig. 2, the workflow mechanism of L₁ is shown.

3.3 Level L₂: Change Detection Types (CDT)

At this level, the 3D city model (along with the semantic, geometric and topological information) has the average backscattering value of the pre-event ($\sigma_{[dB]pre}^0$) and post-event ($\sigma_{[dB]post}^0$) for each building (or selected buildings) in the 3D city model database table. The input required for L₂ is ($\sigma_{[dB]pre}^0$) and post-event ($\sigma_{[dB]post}^0$). At L₂, detailed analysis is performed in order to categorize the change detection types (CDT) into three major types, which are:

- I. CDT₁: Destroyed—the buildings were considered to be affected by the disaster if

$$\sigma_{[dB]pre}^0 > \sigma_{[dB]post}^0$$

The level L₃ will be executed if and only if CDT₁ is true.

- II. CDT₂: No change—the building (or area) is safe from the disaster if

$$\sigma_{[dB]pre}^0 \approx \sigma_{[dB]post}^0$$

is true.

- III. CDT₃: New construction—if there is an empty plot next to a building $b_1 \in \{the\ existing\ 3D\ citymodel\}$, one can confirm that this area (plot) is still empty or whether if there is a new building in that plot. If the condition

$$(\sigma_{[dB]pre}^0 - \sigma_{[dB]post}^0) > -5[dB]$$

is true, that is an indicator for urbanization or new construction. The average radar signal backscattering from man-made structures (urban) is greater than -5 (dB) (Dekker 2010), so this finding can be integrated to detect urbanization. Figure 2 describes the workflow of L₂.

3.4 Level L₃: Prediction

Following the identification of the affected areas (CDT₁), we used an interval-valued fuzzy soft set theory based algorithm proposed by [Feng et al. \(2010\)](#) with some modification to predict the most affected building. Figure 2 illustrates the workflow of L₃. In Sect. 4, we showed the potential application of *interval-valued fuzzy soft sets* for the prediction of the scale of damage. In Sect. 5.3.2, an example application (based on hypothetical data) of this level is shown.

4 Implementation Scheme

Before implementing this conceptual model, we create two generic attributes, $\sigma_{[dB]pre}^0$ and $\sigma_{[dB]post}^0$, in the building table of the 3D city model database. Here, we assumed that we already have a $\sigma_{[dB]pre}^0$ value taken at time (t_1) for the buildings under investigation. Following the event (earthquake), this (Fig. 3) workflow begins. First, we take the ROIs (building footprints) from the 3D city database and export them to the CityGML file through the CityGML export/import tool. The CityGML file is converted to an ESRI shape file using the FME tool, and the footprints are imported using the conversion function in ArcCatalog (ArcGIS). The footprints of the buildings are integrated (manually checked and parallel layered with the bounding boxes of the same buildings) and then are used to calculate the $\sigma_{[dB]post}^0$ value at acquisition (t_2) for each building. After calculating the $\sigma_{[dB]post}^0$ value for each building, an Excel sheet is generated containing the building ID and

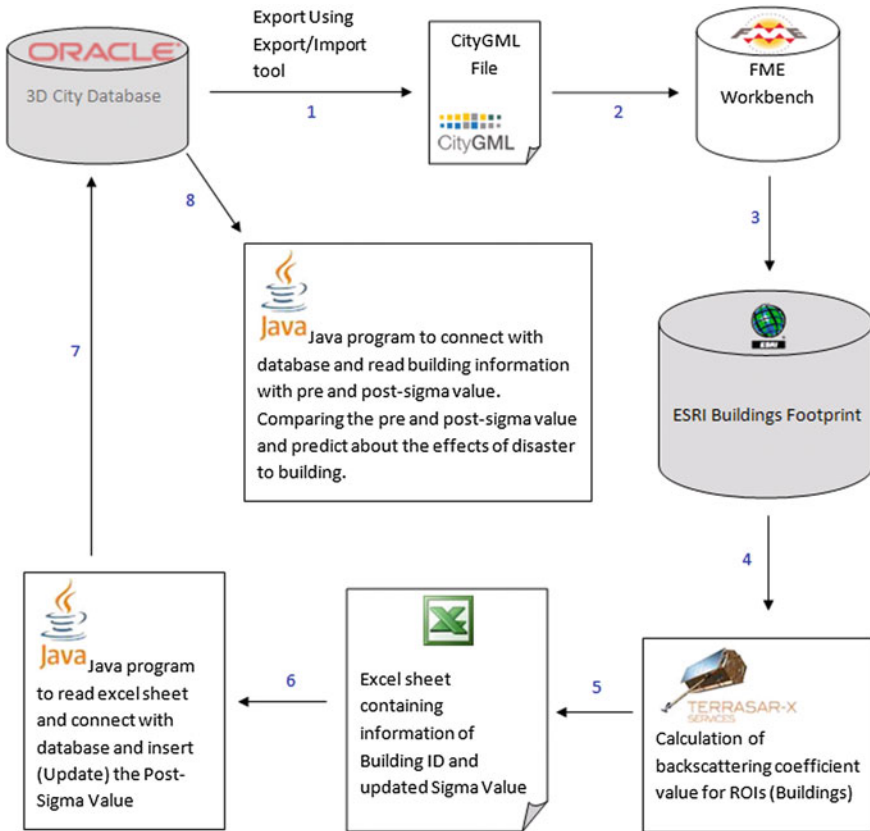


Fig. 3 Implementation scheme

the updated $\sigma_{[\text{dB}]post}^0$ value. Through a Java program, the Excel sheet is read and connected with the 3D city database, and the $\sigma_{[\text{dB}]post}^0$ value for the relevant building is updated. Once the $\sigma_{[\text{dB}]pre}^0$ and $\sigma_{[\text{dB}]post}^0$ values for the buildings of concern are acquired, the program reads both values and classifies the buildings according to the CDT as a final step. The detailed implementation scheme is shown in Fig. 3.

5 Results

5.1 Level L_1 : Space-Borne Data Collection

At this initial level, space-borne pre-event (X_{t_1}) and post-event (X_{t_2}) SAR data were collected and processed as described in Sect. 2. For testing the proposed model, we selected 13 ROIs in the region, and the backscattering coefficients (σ^0) were calculated for both the t_1 and t_2 data sets, which were used as the input ($\sigma_{[\text{dB}]pre}^0, \sigma_{[\text{dB}]post}^0$) into L_2 .

5.2 Level L_2 : Change Detection Types (CDT)

At L_2 , the input ($\sigma_{[\text{dB}]pre}^0, \sigma_{[\text{dB}]post}^0$) values were analyzed in order to classify them into their corresponding CDT categories. Table 2 shows the list of CDT₁ types and the number of cases found for each CDT.

In Fig. 4a, three cases (row wise, D_1, D_2, D_3) of CDT₁ are shown in which structures (buildings) were present in the first acquisition (t_1) and disappeared in the second acquisition (t_2). Figure 5a shows the significant decrease in the $\sigma_{[\text{dB}]post}^0$ value with respect to the $\sigma_{[\text{dB}]pre}^0$ value for these buildings. The $\sigma_{[\text{dB}]post}^0$ values for D_1, D_2 and D_3 decrease by +4.29, +6.58 and +10.32 (dB) respectively in (t_2). CDT₂ is dedicated to the identification of safe buildings or areas that did not change between the X_{t_1} and X_{t_2} acquisitions. Figure 4b shows the five buildings that were found to be safe out of the 13 areas investigated. Figure 5b shows that the $\sigma_{[\text{dB}]pre}^0$ and $\sigma_{[\text{dB}]post}^0$ values are approximately the same for these five buildings. Samples of buildings in order to detect the new constructions, CDT₃ is proposed, where the

Table 2 Categorization of CDT

Classification	CDT_i	No. of cases (K)	Abbreviation
Destroyed	CDT_1	3	$D_i, i = 1, \dots, K$ (where, $K = 3$)
No change	CDT_2	5	$NC_i, i = 1, \dots, K$ (where, $K = 5$)
New construction	CDT_3	5	$N_i, i = 1, \dots, K$ (where, $K = 5$)

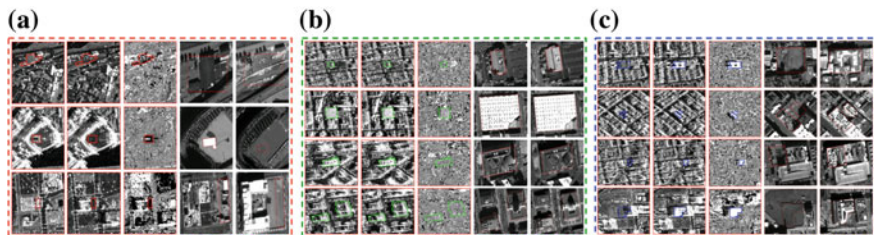


Fig. 4 Columns 1–5 are X_{t_1} , X_{t_2} , X_{LR} , QuickBird (PAN) (t_1) and WorldView-2 (PAN) (t_2) respectively. **a** Rows 1–3 are the three cases which were categorized as CDT_1 ; **(b)** Column 1–5 are X_{t_1} , X_{t_2} , X_{LR} , QuickBird (PAN) (t_1) and WorldView-2 (PAN) (t_2) respectively. Rows 1–4 is the cases that were categorized as CDT_2 ; **(c)** Column 1–5 are X_{t_1} , X_{t_2} , X_{LR} , QuickBird (PAN) (t_1) and WorldView-2 (PAN) (t_2) respectively. Rows 1–4 are the four cases that were categorized as CDT_3

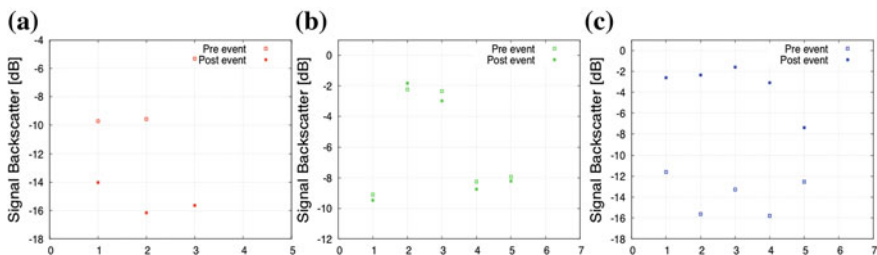


Fig. 5 The mean backscattering value on building footprints, **(a)** CDT_1 : Backscattering coefficient value for three (D_1 , D_2 and D_3) cases as shown in Fig. 4a. **(b)** CDT_2 : Backscattering coefficient value for five cases as shown in Fig. 4b. **(c)** CDT_3 : Backscattering coefficient value for five cases as shown in Fig. 4c

value of $\sigma_{[dB]post}^0$ must be greater than that of $\sigma_{[dB]pre}^0$. Five newly constructed buildings were found in the region, as shown in Fig. 4c. The value of $\sigma_{[dB]post}^0$ for safe buildings (NC) increases by 8:97, 13:27, 11:66, 12:70 and 11:79 (dB) compared with the $\sigma_{[dB]pre}^0$, as shown in Fig. 5c.

5.3 Level L3: Prediction

At L_3 , we proposed the application of interval-valued fuzzy soft sets for the prediction of the scale of damage. This level will be executed if and only if CDT_1 is true for L_2 . In this section, we show the application framework for this procedure with an example demonstration.

5.3.1 Preliminaries: Interval-Valued Fuzzy Soft Sets

Let U be the initial universe and E be the set of parameters. Let $P(U)$ denote the set of all subsets and $A \subseteq E$.

Definition 1 (Maji et al. 2002, Molodtsov 1999) A pair (F, E) is called a *soft set over U* if and only if F is a mapping of E into the set of subsets of the set U (power set $P(U)$), i.e., $F: E \rightarrow P(U)$.

Definition 2 (Maji et al. 2001) A pair (G, A) is called a *fuzzy soft set over U* where G is a mapping of $A \subseteq E$ into the set of all fuzzy subsets in U denoted by $F(U)$), i.e., $G: A \rightarrow F(U)$.

Definition 3 (Yang et al. 2009) An *interval-valued fuzzy set I* on an universe (U) is a mapping such that

$$I:U \rightarrow Int([0, 1])$$

where $Int([0,1])$ stands for the set of all closed subintervals of $([0,1])$, the set of all *interval-valued fuzzy sets* is denoted by $P(U)$.

Definition 4 (Yang et al. 2009) Let U be an initial universe, E be a set of parameters and $A \subseteq E$., a pair (\dot{F}, A) is called an *interval-valued fuzzy soft set (IVFS)* over U , where \dot{F} is a mapping defined as $F : E \rightarrow P(U)$.

Definition 5 (Feng et al. 2010) Let (U, E) be a st universe and $A \subseteq E$. Let (\dot{F}, A) be an (IVFS) over U such that $\forall a \in A, \dot{F}(a)$ is an *interval-valued fuzzy set* with $\dot{F}(a)(x) = [\dot{F}(a)_*(x), \dot{F}(a)^*(x)]$, $\forall x \in U$, where $\dot{F}(a)_*(x)$ and $\dot{F}(a)^*(x)$ are called the lower and upper degrees of membership of x in \dot{F} . Then the fuzzy soft set (\dot{F}, A) over U given by

$$\dot{F}_-(a) = \{(x, \dot{F}(a)_*(x)) : x \in U\}, \quad \forall a \in A$$

is called *pessimistic reduct fuzzy soft set (PRFS)* of (\dot{F}, A) .

Similarly,

$$\dot{F}_+(a) = \{(x, \dot{F}(a)^*(x)) : x \in U\}, \quad \forall a \in A$$

is called *optimistic reduct fuzzy soft set (ORFS)* of (\dot{F}, A) and

$$\dot{F}_N(a) = \{(x, (\dot{F}(a)_*(x) + \dot{F}(a)^*(x))/2) : x \in U\}, \quad \forall a \in A$$

is called *neutral reduct fuzzy soft set (NRFS)* of (\dot{F}, A) .

Definition 6 (Feng et al. 2010) Let (U, E) be soft universe and $A \subseteq E$ and $t \in [0,1]$. The t -level soft set of a fuzzy soft set (\tilde{F}, A) over U is at $(F_t(a))$ defined by

$$(F_t(a)) = \{x \in U: \tilde{F}(a)(x) \geq t\}, \quad \forall a \in A$$

5.3.2 Application Example

Suppose that, following L_2 , we have detected that condition C is true for the following five buildings, $B_i \in \{3D\ CityModelling\}$ (where, $i = 1, 2, \dots, 5$); CDT_1 being true indicates that buildings are affected (or most affected) by the event. We can then predict the most severely affected building among these five buildings and then can be reorded ading to the level of destruction by using level soft sets based on *interval-valued fuzzy soft sets*.

Suppose the following:

- i. $U = \{d_1, d_2, d_3, d_4, d_5\} = \{\text{Five affected buildings}\}$
- ii. $E = \{\varepsilon_1, \varepsilon_2, \varepsilon_3, \varepsilon_4, \varepsilon_5\} = \{\text{magnitude of earthquake, change in } \sigma^0, \text{ age of building, earthquake duration, building original height}\}$. Different It of parameters can also be used according to the present scenario and expert opinion.

Algorithm (Feng et al. 2010; Yang et al. 2009).

1. *Input*: The set of *Interval-valued fuzzy soft sets* defined by using definition 4. In our case *Interval-valued fuzzy soft set* (\tilde{F}, A) is shown in Table 3.
2. *Input*: Parameter set E consists of preferences of decision maker, parameter under consideration in our case are $E = \{\varepsilon_1, \varepsilon_2, \varepsilon_3, \varepsilon_4, \varepsilon_5\} = \{\text{magnitude of earthquake, change in } \sigma^0, \text{ age of building, earthquake duration, building original height}\}$

Table 3 Interval-valued fuzzy soft set (\tilde{F}, A)

U	ε_1	ε_2	ε_3	ε_4	ε_5
d_1	[0.7, 1.0]	[0.5, 0.7]	[0.2, 0.5]	[0.5, 0.6]	[0.7, 0.8]
d_2	[0.6, 0.2]	[0.9, 0.1]	[0.8, 0.9]	[0.5, 0.7]	[0.1, 0.3]
d_3	[1.0, 0.9]	[0.3, 0.6]	[0.6, 0.5]	[0.7, 0.3]	[0.2, 0.9]
d_4	[0.2, 0.8]	[0.7, 0.3]	[0.3, 1.0]	[0.9, 0.1]	[0.4, 0.8]
d_5	[0.4, 0.2]	[0.4, 0.5]	[0.5, 0.8]	[0.6, 0.1]	[0.9, 0.3]

Table 4 Pessimistic reduct fuzzy soft set (PRFS) of (\dot{F}, A)

U	ε_1	ε_2	ε_3	ε_4	ε_5
d_1	0.7	0.5	0.2	0.5	0.7
d_2	0.2	0.1	0.8	0.5	0.1
d_3	0.9	0.3	0.5	0.3	0.2
d_4	0.2	0.3	0.3	0.1	0.4
d_5	0.2	0.4	0.5	0.1	0.3

Table 5 Optimistic reduct fuzzy soft set (ORFS) of (\dot{F}, A)

U	ε_1	ε_2	ε_3	ε_4	ε_5
d_1	1.0	0.7	0.5	0.6	0.8
d_2	0.6	0.9	0.9	0.7	0.3
d_3	1.0	0.6	0.6	0.7	0.9
d_4	0.8	0.7	1.0	0.9	0.8
d_5	0.4	0.5	0.8	0.6	0.9

Table 6 Neutral reduct fuzzy soft set (NRFS) of (\dot{F}, A)

U	ε_1	ε_2	ε_3	ε_4	ε_5
d_1	0.85	0.60	0.35	0.55	0.75
d_2	0.40	0.50	0.85	0.60	0.20
d_3	0.95	0.45	0.55	0.50	0.55
d_4	0.50	0.50	0.65	0.50	0.60
d_5	0.30	0.45	0.65	0.35	0.60

3. *Compute*: By using definition 5 calculate $\dot{F}_-(a), \forall a \in A$ (PRFS), $\dot{F}_+(a), \forall a \in A$ (ORFS) and $\dot{F}_N(a), \forall a \in A$ (NRFS) which are shown in Table 4, Table 5 and Table 6 respectively.
4. *Compute*: $\forall d_i \in U$, compute the interval fuzzy choice value c_i for each damage type d_i such that

$$c_i = [c_i^-, c_i^+] = \left[\sum_{a \in A \subseteq E} \dot{F}_-(a)(d_i), \sum_{a \in A \subseteq E} \dot{F}_+(a)(d_i) \right]$$

Table 7 shows the choice values for each d_i .

5. *Compute*: $\forall d_i \in U$, compute the score value r_i for each d_i such that

$$r_i = \sum_{d_i \in U} \left((c_i^- - c_j^-) + (c_i^+ - c_j^+) \right)$$

Table 7 Choice values and scores

U	c_i	r_i
d_1	$c_1 = [2.6, 3.6]$	$r_1 = 3.3$
d_2	$c_2 = [1.7, 3.4]$	$r_2 = -2.0$
d_3	$c_3 = [2.2, 3, 8]$	$r_3 = 2.9$
d_4	$c_4 = [1.3, 4.2]$	$r_4 = 0.0$
d_5	$c_5 = [1.5, 3.2]$	$r_5 = -4.0$

Table 7 shows the score values for each d_i .

6. Decision: Selection of $d_m \in U$ with maximum score value i.e., $r_m = \max_{d_i \in U} \{r_i\}$.
As shown in

Table 7 $r_1 > r_i$, where $i = 2, 3, 4, 5$. Finally $\{d_1\}$ has the maximum score.

7. Threshold value t: We define the threshold values t on membership degree as follow

$$t = \frac{\sum_{j=1}^N \left(\frac{\sum_{i=1}^N a_{ij}}{N} \right)}{N}$$

where, $t \in [0,1]$ and from Table 5 we get $t = 0.55$.

8. Compute: Computation of level soft set with $t = 0.55$ by applying definition 6 in Table 6, results are shown in Table 8.
9. Decision: By considering the aggregation $G = \max$, from Table 4 threshold fuzzy set is induced which is

$$\tilde{g} = \{\varepsilon_1 = 0.9, \varepsilon_2 = 0.5, \varepsilon_3 = 0.8, \varepsilon_4 = 0.5, \varepsilon_5 = 0.7\}$$

By using these fuzzy thresholds top-level crisp soft set is obtain as shown in Table 9. $c_1 > c_i$, where $i = 2, 3, 4, 5$. Finally d_1 has the maximum choice value.

Table 8 Level soft set with $t = 0.55$

U	ε_1	ε_2	ε_3	ε_4	ε_5
d_1	1	1	0	1	1
d_2	0	0	1	1	0
d_3	1	0	1	0	1
d_4	0	0	1	0	1
d_5	0	0	1	0	1

Table 9 Level soft set (max)

U	ε_1	ε_2	ε_3	ε_4	ε_5	c_i
d_1	0	1	0	1	1	$c_1 = 3.0$
d_2	0	0	1	1	0	$c_2 = 2.0$
d_3	1	0	0	0	0	$c_3 = 1.0$
d_4	0	0	0	0	0	$c_4 = 0.0$
d_5	0	0	0	0	0	$c_5 = 0.0$

6 Discussion

Considering the possible future disaster threats to highly vulnerable cities, Kubal et al. (2009) used a multi-criterion approach for urban flood risk assessment. The proposed model is highly feasible for implementation and for operational search and rescue activities. The weather independence, day-night imaging capability and short revisit time of current (and future) SAR-sensors demonstrate the feasibility of implementation of this model. The proposed model has great potential to extend the database and to record the earthquake resistant history for each building. Several authors have proposed different change detection techniques that use only optical, SAR or laser scanning data. One might question the purpose of using SAR data in combination with 3D city models. For example, if an earthquake occurs on Sunday morning, then the affected areas (buildings) can be found by using SAR data; however, the important question is how to determine the priorities for rescue teams. During weekends, university, school, college, and office buildings are closed; thus, by using the semantic information query from the 3D city model, such buildings can easily be filtered out, and the focus and resources can be shifted towards the residential and other affected areas.

The advantage of using a 3D city model in combination with SAR data is that, once an affected building is identified, the rescue teams can be assisted accordingly by using the geometric and topological consistency (Gröger and Plümer 2012) information from the 3D model. For example, by analyzing the geometry and topological properties of the building (3D model), one can guide the rescue teams in real time with respect to the types of cutters, jacks or hydraulic cranes (small or large) that might be needed to rescue trapped people. Another major advantage of the combined use of an existing 3D city model database and SAR remote sensing is that the SAR change detection information can be further filtered and classified based on the 3D city model semantic information. For example, in our case, we have three buildings (D_1 , D_2 and D_3) that were found to be destroyed as a result of the SAR change detection (CDT_2); by using the 3D city model semantic information, we can further query whether each building belongs to such categories as public schools, hotels, residential, or trade/office buildings. Thus, in large-scale disasters, limited resources can be used more efficiently, and search and rescue operations can be performed in a more targeted and focused manner.

Kolbe et al. (2005) (sec. 4: Application of CityGML for Disaster Management) showed that thematically rich attributes effectively allow specific queries during

emergencies, allowing queries such as “Where are buildings with flat roofs that are large enough for a helicopter to land?” (Kolbe et al. 2005). However after an earthquake of magnitude of 8 or 9, how do we know that these buildings with flat roofs are still safe and did not collapse?” the answer will come from L2 of our proposed model and will allow more efficient relief and rescue operations. This query can now be rephrased for an emergency as, *Where are buildings with flat roofs with $\sigma_{[dB]pre}^0 \approx \sigma_{[dB]post}^0$ (safe) that are large enough for a helicopter to land?*

The application scale of this framework could be on a local (district or town) or city level; for example, the city of Berlin can be covered by a single TerraSAR-X StripMap scene [up to 3 m resolution, with a scene size of 30 km (width) \times 50 km (length)]. This method is suitable for most cities and sites that are vulnerable to disasters. For example, Pakistan and India have military check posts on Siachen Glacier (located in the eastern Karakoram range in the Himalaya Mountains), where landslides and avalanches are quite frequent. A recent tragedy occurred in the Gyari sector of Pakistan in which 139 soldiers and civilians were buried under 80 feet of snow, when a huge avalanche hit a military base at the foot of Siachen glacier. The search and rescue teams faced difficulties in locating the exact site of the base camp; owing to the cloudy weather of the mountainous region, the acquisition of optical imagery is not always possible. Because of the huge amount of debris and snow, a more precise digging process was required. In such a situation, our proposed methodology could overcome these limitations. Similarly, in an urban environment, the proposed technique could be installed and used for the precise identification of potentially damaged areas and the estimation of the scale of damage to allow more precise and targeted search and rescue operations.

By using SAR remote sensing following a disaster event, we can precisely find the exact location (L), and then by using the semantic information from an existing 3D virtual model, we can plan more precise and efficient search and rescue operations. Figure 6 describes the possible schema for post-disaster planning using the semantic information from a 3D model. For example, in such a case, tunnel T_d^h from the west with diameter d and height h would be the best choice because there is a high probability of finding bodies in area (A) near or around the main entrance (door).

7 Conclusion and Future Work

We have proposed a new model for rapid post disaster management and emergency response. Our proposed approach has good potential to meet future needs in the field of disaster management as a decision support system. By focusing on the current developments in the fields of science and technology, we can imagine how cities could be managed and organized in the future. We have proposed a new model for monitoring urban areas for both positive (new construction) and negative (building destruction) changes by using SAR data in combination with a 3D city

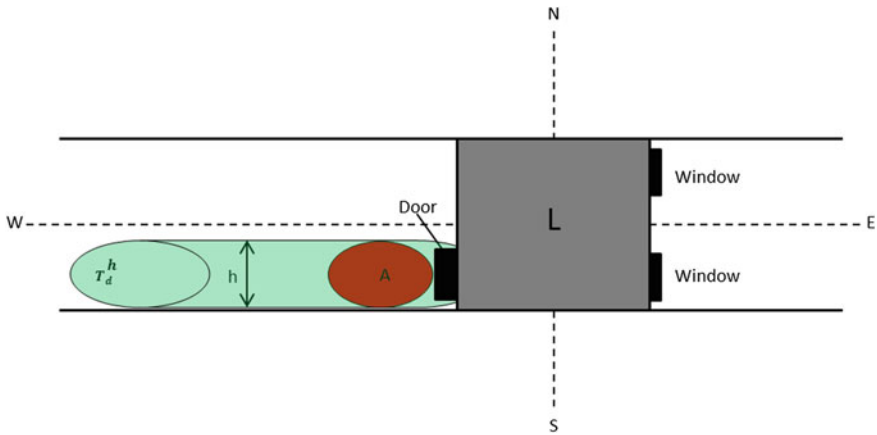


Fig. 6 Planning framework based on semantic 3D building model

model database. We have discussed how semantic information from 3D city models can be used effectively for rapid post disaster management activities. To manage the uncertainties and to predict the scale of damage, the application of *interval-valued fuzzy soft sets* is implemented. The initial results show that the proposed model is highly feasibility and effective. In the future, the proposed model could be effectively used at a large scale for relief and rescue activities in modern cities.

Despite the fact that $\sigma_{[dB]post}^0$ will decrease for damage buildings as compare to the non-damage buildings (Matsuoka and Yamazaki 2004a, b), but still there are some other issues related to SAR geometric distortions (shadow, layover) and backscattering behavior are very important that need to be handled carefully. Specular scattering from the flat roof tops (multiple adjacent buildings) and could

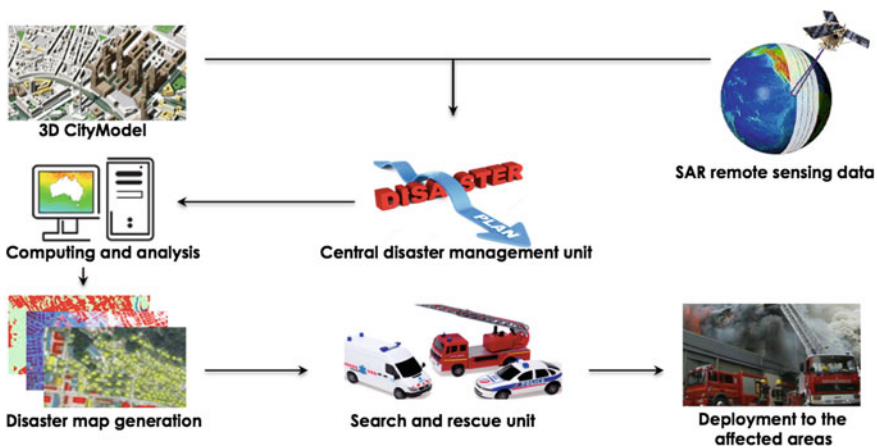


Fig. 7 Graphical abstract of the proposed methodology

cause a lambertian scattering from the collapsed building and could create a relatively high backscattering as compare to the flat roof surface (Matsuoka and Yamazaki 2004a, b). The use of multi-sensor remote sensing can be used for the identification of damaged areas (Wang and Jin 2012). For level L_2 any remote sensing data and change detection algorithm can be used and the rule ($\sigma_{[dB]pre}^0 > \sigma_{[dB]post}^0$) can be redefined accordingly. After going through the work done by Brunner et al. (2009, 2010) we believe that his approach for earthquake damage assessment is most feasible to be used for change detection at level L_2 . The Fig. 7 shows the graphical overview (big picture) of the proposed approach.

Acknowledgments The authors would like to thank DigitalGlobe, Astrium Services, and USGS for providing the remote sensing data used in this study and the IEEE GRSS Data Fusion Technical Committee for organizing the Data Fusion Contest.

References

- Brunner D (2009) Advanced methods for building information extraction from very high resolution SAR data to support emergency response. Ph.D., University of Trento, Trento, Italy
- Brunner D, Lemoine G, Bruzzone L (2010) Earthquake damage assessment of buildings using VHR optical and SAR imagery. *IEEE Trans Geosci Remote Sens* 48:2403–2420. doi:10.1109/TGRS.2009.2038274
- Chetia B, Das PK (2010) An application of interval-valued fuzzy soft sets in medical diagnosis. *Int J Contemp Math Sci* 5:1887–1894
- CityGML (2014) <http://www.citygml.org>. Accessed 4.24.14
- Dekker PL (2010) Introduction to SAR [WWW Document]. <https://earth.esa.int/web/guest/training-packages/-/article/esa-polish-academy-of-science-dlr-radar-remote-sensing-course-warsaw>. Accessed 7.25.14
- Dell’Acqua F, Gamba P (2012) Remote sensing and earthquake damage assessment: experiences, limits, and perspectives. *Proc IEEE* 100:2876–2890. doi:10.1109/JPROC.2012.2196404
- Dell’Acqua F, Gamba P, Polli D (2010) Mapping earthquake damage in VHR radar images of human settlements: preliminary results on the 6th April 2009, Italy case. In: Geoscience and remote sensing symposium (IGARSS) 2010 IEEE International, pp 1347–1350. doi:10.1109/IGARSS.2010.5653973
- Dell’Acqua F, Lisini G, Gamba P (2009) Experiences in optical and SAR imagery analysis for damage assessment in the Wuhan, may 2008 earthquake. In: IEEE international geoscience and remote sensing symposium 2009, IGARSS 2009, pp IV–37, IV–40. doi:10.1109/IGARSS.2009.5417603
- Dong L, Shan J (2013) A comprehensive review of earthquake-induced building damage detection with remote sensing techniques. *ISPRS J Photogramm Remote Sens* 84:85–99. doi:10.1016/j.isprsjprs.2013.06.011
- Feng F, Li Y, Leoreanu-Fotea V (2010) Application of level soft sets in decision making based on interval-valued fuzzy soft sets. *Comput Math Appl* 60:1756–1767. doi:10.1016/j.camwa.2010.07.006
- Gröger G, Kolbe T, Czerwinski A, Nagel C (2008) Open GIS city geography markup language (CityGML) encoding standard (OGC 08-007r1)
- Gröger G, Plümer L (2012) Provably correct and complete transaction rules for updating 3D city models. *GeoInformatica* 16:131–164. doi:10.1007/s10707-011-0127-6

- Kagan YY (1997) Are earthquakes predictable? *Geophys J Int* 131:505–525. doi:[10.1111/j.1365-246X.1997.tb06595.x](https://doi.org/10.1111/j.1365-246X.1997.tb06595.x)
- Kolbe TH (2009) Representing and exchanging 3D city models with city GML. In: Lee J, Zlatanova S (eds) *3D Geo-information sciences. Lecture notes in geoinformation and cartography*. Springer, Berlin Heidelberg, pp 15–31
- Kolbe TH, Gröger G, Plümer L (2005) CityGML: interoperable access to 3D city models. In: van Oosterom PDP, Zlatanova DS, Fendel EM (eds) *Geo-information for disaster management*. Springer, Berlin, Heidelberg, pp 883–899
- Kubal C, Haase D, Meyer V, Scheuer S (2009) Integrated urban flood risk assessment—adapting a multicriteria approach to a city. *Nat Hazards Earth Syst Sci* 9:1881–1895. doi:[10.5194/nhess-9-1881-2009](https://doi.org/10.5194/nhess-9-1881-2009)
- Lu D, Mausel P, Brondizio E, Moran E (2004) Change detection techniques. *Int J Remote Sens* 25:2365–2401. doi:[10.1080/0143116031000139863](https://doi.org/10.1080/0143116031000139863)
- Lu W, Doihara T, Matsumoto Y (1998) Detection of building changes by integration of aerial imageries and digital maps. *Int Arch Photogram Remote Sens* 32:244–347
- Maji PK, Biswas R, Roy AR (2001) Fuzzy soft sets. *Fuzzy Math* 9:589–602
- Maji PK, Roy AR, Biswas R (2002) An application of soft sets in a decision making problem. *Comput Math Appl* 44:1077–1083. doi:[10.1016/S0898-1221\(02\)00216-X](https://doi.org/10.1016/S0898-1221(02)00216-X)
- Martin R, Bernhard H (2010) Change detection of building footprints from airborne laser scanning acquired in short time intervals. Presented at the ISPRS commission VII mid-term symposium 100 Years ISPRS—advancing remote sensing science, Vienna, Austria, pp 475–480
- Matsuoka M, Yamazaki F (2004a) Use of satellite SAR intensity imagery for detecting building areas damaged due to earthquakes. *Earthq Spectra* 20:975–994. doi:[10.1193/1.1774182](https://doi.org/10.1193/1.1774182)
- Matsuoka M, Yamazaki F (2004) Building damage detection using satellite SAR intensity images for the 2003 Algeria and Iran earthquakes. In: IEEE international geoscience and remote sensing symposium 2004, IGARSS '04, pp. 1099–1102. doi:[10.1109/IGARSS.2009.5417603](https://doi.org/10.1109/IGARSS.2009.5417603)
- Molodtsov D (1999) Soft set theory—first results. *Comput Math Appl* 37:19–31. doi:[10.1016/S0898-1221\(99\)00056-5](https://doi.org/10.1016/S0898-1221(99)00056-5)
- Murakami H, Nakagawa K, Hasegawa H, Shibata T, Iwanami E (1999) Change detection of buildings using an airborne laser scanner. *ISPRS J Photogramm Remote Sens* 54:148–152. doi:[10.1016/S0924-2716\(99\)00006-4](https://doi.org/10.1016/S0924-2716(99)00006-4)
- Park S-E, Yamaguchi Y, Kim D (2013) Polarimetric SAR remote sensing of the 2011 Tohoku earthquake using ALOS/PALSAR. *Remote Sens Environ* 132:212–220. doi:[10.1016/j.rse.2013.01.018](https://doi.org/10.1016/j.rse.2013.01.018)
- Suga Y, Takeuchi S, Oguro Y, Chen AJ, Ogawa M, Konishi T, Yonezawa C (2001) Application of ERS-2/SAR data for the 1999 Taiwan earthquake. *Adv Space Res* 28:155–163. doi:[10.1016/S0273-1177\(01\)00334-9](https://doi.org/10.1016/S0273-1177(01)00334-9)
- Tong X, Lin X, Feng T, Xie H, Liu S, Hong Z, Chen P (2013) Use of shadows for detection of earthquake-induced collapsed buildings in high-resolution satellite imagery. *ISPRS J Photogramm Remote Sens* 79:53–67. doi:[10.1016/j.isprsjprs.2013.01.012](https://doi.org/10.1016/j.isprsjprs.2013.01.012)
- Trianni G, Gamba P (2009) Fast damage mapping in case of earthquakes using multitemporal SAR data. *J Real-Time Image Process* 4:195–203. doi:[10.1007/s11554-008-0108-7](https://doi.org/10.1007/s11554-008-0108-7)
- Vogtle T, Steinle E (2004) Detection and recognition of changes in building geometry derived from multitemporal laserscanning data. Presented at the International Archives of Photogrammetry, Remote Sens Spat Inf Sci, Istanbul, Turkey, pp 428–433
- Wang T-L, Jin Y-Q (2012) Postearthquake building damage assessment using multi-mutual information from pre-event optical image and postevent SAR image. *IEEE Geosci Remote Sens Lett* 9:452–456. doi:[10.1109/LGRS.2011.2170657](https://doi.org/10.1109/LGRS.2011.2170657)
- Yang X, Lin TY, Yang J, Li Y, Yu D (2009) Combination of interval-valued fuzzy set and soft set. *Comput Math Appl* 58:521–527. doi:[10.1016/j.camwa.2009.04.019](https://doi.org/10.1016/j.camwa.2009.04.019)